

ORIGINAL RESEARCH

# Differential Downregulation of $\beta_1$ -Adrenergic Receptor Signaling in the Heart

Bing Xu , BS; Sherif Bahriz , MD; Victoria R. Salemme , MS; Ying Wang, PhD; Chaoqun Zhu , PhD; Meimi Zhao, PhD; Yang K. Xiang , PhD

**BACKGROUND:** Chronic sympathetic stimulation drives desensitization and downregulation of  $\beta_1$  adrenergic receptor ( $\beta_1$ AR) in heart failure. We aim to explore the differential downregulation subcellular pools of  $\beta_1$ AR signaling in the heart.

**METHODS AND RESULTS:** We applied chronic infusion of isoproterenol to induced cardiomyopathy in male C57BL/6J mice. We applied confocal and proximity ligation assay to examine  $\beta_1$ AR association with L-type calcium channel, ryanodine receptor 2, and SERCA2a ((Sarco)endoplasmic reticulum calcium ATPase 2a) and Förster resonance energy transfer-based biosensors to probe subcellular  $\beta_1$ AR-PKA (protein kinase A) signaling in ventricular myocytes. Chronic infusion of isoproterenol led to reduced  $\beta_1$ AR protein levels, receptor association with L-type calcium channel and ryanodine receptor 2 measured by proximity ligation (puncta/cell, 29.65 saline versus 14.17 isoproterenol,  $P<0.05$ ), and receptor-induced PKA signaling at the plasma membrane (Förster resonance energy transfer, 28.9% saline versus 1.9% isoproterenol,  $P<0.05$ ) and ryanodine receptor 2 complex (Förster resonance energy transfer, 30.2% saline versus 10.6% isoproterenol,  $P<0.05$ ). However, the  $\beta_1$ AR association with SERCA2a was enhanced (puncta/cell, 51.4 saline versus 87.5 isoproterenol,  $P<0.05$ ), and the receptor signal was minimally affected. The isoproterenol-infused hearts displayed decreased PDE4D (phosphodiesterase 4D) and PDE3A and increased PDE2A, PDE4A, and PDE4B protein levels. We observed a reduced role of PDE4 and enhanced roles of PDE2 and PDE3 on the  $\beta_1$ AR-PKA activity at the ryanodine receptor 2 complexes and myocyte shortening. Despite the enhanced  $\beta_1$ AR association with SERCA2a, the endogenous norepinephrine-induced signaling was reduced at the SERCA2a complexes. Inhibiting monoamine oxidase A rescued the norepinephrine-induced PKA signaling at the SERCA2a and myocyte shortening.

**CONCLUSIONS:** This study reveals distinct mechanisms for the downregulation of subcellular  $\beta_1$ AR signaling in the heart under chronic adrenergic stimulation.

**Key Words:** (Sarco)endoplasmic reticulum calcium ATPase 2a ■ cardiac contractility ■ Förster resonance energy transfer ■ phosphodiesterase ■ protein kinase a ■ ryanodine receptor ■  $\beta_1$  adrenergic receptor

Adrenergic signaling is downregulated in various cardiac diseases, a hallmark of heart failure (HF). In classic literature, the primary cardiac  $\beta_1$  adrenergic receptor ( $\beta_1$ AR) undergoes desensitization via receptor phosphorylation driven by chronic sympathetic activation, which uncouples the receptor from G proteins and scaffold proteins such as SAP97 (synapse-associated protein-97) and AKAP (A-kinase anchoring protein).<sup>1-3</sup> Interestingly, we have recently identified a novel pool of intracellular  $\beta_1$ AR specifically associated

with SERCA2a ((Sarco)endoplasmic reticulum calcium ATPase 2a), critical for catecholamine stimulation of excitation-contraction coupling and cardiac contractility.<sup>4-6</sup> Here, we aimed to understand how chronic adrenergic stimulation affects the subcellular pools of  $\beta_1$ AR signaling in cardiomyopathy.

Stimulation of  $\beta_1$ AR promotes PKA (protein kinase A) phosphorylation and increases the activities of L-type calcium channel (LTCC), ryanodine receptor 2 (RyR2), and SERCA2a, critical ion regulators to enhance

Correspondence to: Yang K. Xiang, PhD, Department of Pharmacology, University of California, Davis, One Shields Avenue, Davis, CA 95616-8636. Email: [ykxiang@ucdavis.edu](mailto:ykxiang@ucdavis.edu)

This article was sent to Sakima A. Smith, MD, MPH, Associate Editor, for review by expert referees, editorial decision, and final disposition.

Supplemental Material is available at <https://www.ahajournals.org/doi/suppl/10.1161/JAHA.123.033733>

For Sources of Funding and Disclosures, see page 16.

© 2024 The Authors. Published on behalf of the American Heart Association, Inc., by Wiley. This is an open access article under the terms of the [Creative Commons Attribution-NonCommercial-NoDerivs](https://creativecommons.org/licenses/by-nc-nd/4.0/) License, which permits use and distribution in any medium, provided the original work is properly cited, the use is non-commercial and no modifications or adaptations are made.

JAHA is available at: [www.ahajournals.org/journal/jaha](http://www.ahajournals.org/journal/jaha)

## RESEARCH PERSPECTIVE

### What Is New?

- Chronic stimulation reduced cardiac  $\beta_1$  adrenergic receptor expression and signaling associated with L-type calcium channel and ryanodine receptor complexes, which were also controlled by PDE2 (phosphodiesterase 2) and PDE3.
- Although norepinephrine-induced cardiac  $\beta_1$  adrenergic receptor signaling at the SERCA2a ((Sarco)endoplasmic reticulum calcium ATPase 2a) complexes is reduced in myocytes from mice after chronic infusion of isoproterenol, inhibiting MAO-A (monoamino oxidase A) rescues the norepinephrine-induced  $\beta_1$  adrenergic receptor signaling at the SERCA2a complexes, PKA (protein kinase A) phosphorylation of phospholamban, and excitation-contraction coupling.

### What Question Should Be Addressed Next?

- Future studies should address how the subcellular cardiac  $\beta_1$  adrenergic receptor is altered in other cardiac disease models and whether inhibition of MAO-A is effective in rescuing excitation-contraction coupling in human heart failure.

## Nonstandard Abbreviations and Acronyms

<b>AKAP</b>	A-kinase anchoring protein
<b>AKAR</b>	A-kinase activity reporter
<b>AVM</b>	adult ventricular myocyte
<b><math>\beta_1</math>AR</b>	$\beta_1$ adrenergic receptor
<b>CFP</b>	cyan fluorescent protein
<b>CGP</b>	CGP 20712A
<b>EHNA</b>	erythro-9-(2-hydroxy-3-nonyl)adenine
<b>FKBP</b>	FK506 binding protein 12.6
<b>FRET</b>	Förster resonance energy transfer
<b>ICI</b>	ICI-118551
<b>LTCC</b>	L-type calcium channel
<b>MAO-A</b>	monoamino oxidase A
<b>PDE</b>	phosphodiesterase
<b>PKA</b>	protein kinase A
<b>PLB</b>	phospholamban
<b>PM</b>	plasma membrane
<b>RyR</b>	ryanodine receptor
<b>SERCA2a</b>	(Sarco)endoplasmic reticulum calcium ATPase 2a
<b>SR</b>	sarcoplasmic reticulum
<b>YFP</b>	yellow fluorescent protein

cardiac excitation-contraction coupling during stress response.<sup>7,8</sup> RyR2 is closely coupled to LTCC at the tubular membrane and releases calcium from the sarcoplasmic reticulum (SR) to the cytoplasm to enhance excitation-contraction coupling. Conversely, SERCA2a is modulated by a negative regulator, PLB (phospholamban), and is responsible for calcium uptake during cardiac relaxation. Both RyR2 and PLB are regulated by PKA phosphorylation under adrenergic stimulation. Recent studies highlight distinct local signaling based on the distribution of the  $\beta_1$ AR, AKAP scaffold proteins, and downstream effectors such as LTCC, RyR2, and SERCA2a.<sup>4,9-12</sup> Whereas the  $\beta_1$ AR is associated with LTCC on the plasma membrane (PM), a second pool of  $\beta_1$ AR is associated with SERCA2a at the SR.<sup>4-6</sup> PKA is anchored on different AKAPs to promote local phosphorylation of RyR2 and PLB to increase ion channel and pump activities.<sup>7,8</sup> Additionally, PDEs (phosphodiesterases) emerge as critical regulators to fine-tune adrenergic-induced local cAMP and PKA activity at distinct subcellular compartments.<sup>13-16</sup> RyR2 is associated with PDE4D3 and scaffold proteins such as muscle-specific AKAP.<sup>17,18</sup> In comparison, AKAP18 $\delta$ , PDE3, and PDE4 are linked to the SERCA2a.<sup>18-21</sup> How the subcellular  $\beta_1$ AR-PKA signaling is remodeled in heart diseases is incompletely understood.

In this study, we aimed to investigate subcellular adrenergic signaling remodeling in cardiomyopathy with a chronic infusion of  $\beta$ -agonist isoproterenol. We used proximity ligation assay to examine the  $\beta_1$ AR association with LTCC, RyR2, and SERCA2a in isolated adult ventricular myocytes (AVMs). We also applied Förster resonance energy transfer (FRET) biosensors-based AKARs (A-kinase activity reporters)<sup>22-24</sup> to examine PKA activity at the RyR2 and SERCA2a complexes in AVMs. We further assess the impacts of altered  $\beta_1$ AR-PKA signaling on cardiac excitation-contraction coupling in the cardiomyopathy induced by chronic isoproterenol infusion. Our data highlight distinct mechanisms underlying the downregulation of subcellular  $\beta_1$ AR-PKA signaling in AVMs after chronic adrenergic stress in the heart.

## METHODS

### Data Availability

The authors declare that all supporting data are available within the article and its online supplementary files.

### Animals

All animal studies were approved by the Institutional Animal Care and Use Committees (protocol number: 20956 and 20957) of the University of California at Davis according to the National Institutes of Health and Animal Research: Reporting of In Vivo Experiments guidelines.

Male C57BL/6J mice were purchased from Jackson Laboratory (Sacramento, CA); 10- to 12-week-old mice (15/group) were used in chronic infusion of isoproterenol to induce cardiomyopathies or saline as control.<sup>25,26</sup> Animals were housed in cages in a room with controlled temperature, humidity, and 12-12-hour light–dark cycle. Animals developing cardiomyopathy were monitored daily and terminated when reaching human end point. After anesthesia with inhalation of 2.0% isoflurane and oxygen, mice were euthanized to harvest hearts. All studies were randomized and blinded for data analysis. All samples or animals were included in the analysis.

## Reagents

All reagents were obtained from Millipore-Sigma (St. Louis, MO).  $\beta$ -adrenergic agonist, isoproterenol (100 nmol/L) was applied to cultured mouse myocytes with a  $\beta_1$ AR antagonist (CGP 20712A, 300 nmol/L) or a  $\beta_2$ AR antagonist (ICI 118551, 100 nmol/L). Forskolin (10  $\mu$ mol/L) and isobutylmethylxanthine (100  $\mu$ mol/L) were used to activate cAMP and PKA in myocytes maximally. Inhibitor of PDE4 rolipram (10  $\mu$ mol/L), PDE2 erythro-9-(2-hydroxy-3-nonyl)adenine (10  $\mu$ mol/L), and PDE3 cilostamide (1  $\mu$ mol/L) were also used as indicated. Calcium indicator fluo-4 AM (2–5  $\mu$ mol/L, Thermo Fisher Scientific, Waltham, MA) was used to measure calcium transient. All 3 PKA activity biosensors, PM-AKAR3, SR-AKAR3, and FKBP (FK506 binding protein)-AKAR3, have been extensively characterized previously.<sup>22,23,27</sup> FKBP-AKAR3 was generated by fusing AKAR3 to the C-terminus of FKBP12.6. SR-AKAR3 was generated by fusing AKAR3 to the C-terminus of monomerized PLB, whereas PM-AKAR3 was generated by fusing the CAAX membrane targeting sequence KKKKSKTKCVM to the C-terminus of AKAR3 described previously.<sup>22,23,27</sup> The AKAR3 cDNAs were then subcloned into pshuttle vector to generate recombinant padeasy vector for making adenovirus. Adenoviruses containing the AKAR3 fusion genes were made and further amplified in HEK293 cells. The recombinant was purified with a CsCl gradient. We successfully produced the adenoviruses with a titer of  $10^{10}$  to  $10^{12}$  pfu/mL.<sup>22,23,27</sup>

## Transthoracic Echocardiography

Animals were anesthetized with inhaled isoflurane (1%–1.5%) via a nose cone for transthoracic echocardiography. The mice were placed on the platform of the Vevo 2100 imaging system (VisualSonics, Toronto, ON, Canada) in the supine position. The ECG, body temperature, and respiration rate were measured while maintaining the heart rate at around 450 beats per minute. A 22 to 55 MHz linear probe (MS550D) was used to collect the 2-dimensional short-axis projection images.<sup>3,25</sup> Systolic heart function parameters were analyzed in at least 3 heartbeats from each image in a blinded fashion.

## Adult Ventricular Cardiomyocytes Isolation From Adult Mice

AVMs were isolated as previously described.<sup>3,25,28</sup> The anesthesia of mice was induced by 2% isoflurane. The isolated heart was cannulated to a Langendorf perfusion system. The heart was perfused with the digestion buffer (NaCl 120 mmol/L,  $\text{NaH}_2\text{PO}_4$  1.2 mmol/L, KCl 5.4 mmol/L,  $\text{MgSO}_4$  1.2 mmol/L,  $\text{NaHCO}_3$  20 mmol/L, glucose 5.6 mmol/L, taurine 20 mmol/L, 2,3-butanedione monoxime 10 mmol/L, PH7.4). Subsequently, the heart was perfused with the buffer containing collagenase and protease (predigestion solution: 0.05% type II collagenase (Worthington Biochemical, Lakewood, NJ), 0.01% type XIV protease (Sigma-Aldrich), and 0.1% BSA; digestion solution: 0.2% type II collagenase, 0.04% type XIV protease, 50  $\mu$ mol/L  $\text{CaCl}_2$ , and 0.1% BSA). The isolated myocytes were harvested from digestion buffer. Isolated AVMs were used for Western blotting, calcium transient and sarcomere shortening recording, proximity ligation assays, and FRET assays.

## Western Blotting

AVMs from saline and isoproterenol-induced mice were treated with rolipram (10  $\mu$ mol/L, Sigma-Aldrich) for 10 minutes. Alternatively, AVMs were treated with rolipram and isoproterenol (100 nmol/L) stimulation for 10 minutes to detect the effects of rolipram on isoproterenol-induced phosphorylation of PLB and RyR. The treated AVMs or heart tissues from indicated mice were lysed with RIPA buffer supplement with proteinase and phosphatase inhibitors. Immunoblotting was applied to detect the phospho-RyR at Ser2808 (ab59225, Abcam, Cambridge, MA), phospho-RyR at Ser2814 (pRyRS2814, A010-31AP, Badrilla, Leeds, UK), RyR (MA3-925, ThermoFisher, IL),  $\beta_1$ AR (sc-568, Santa Cruz, Dallas, TX), PDE4D (ab14613, Abcam, Cambridge, MA), PLB (A010-14, Badrilla, Leeds, UK), phospho-PLB at Ser16 (pPLBS16, A010-12AP, Badrilla, Leeds, UK), phospho-PLB at Thr17 (pPLBT17, A010-13AP, Badrilla, Leeds, UK), SERCA2a (MA3-911, Thermo Fisher Scientific, Waltham, MA), PDE3A (kind gifts from Yan Chen at University of Rochester), PDE4A and PDE4B (kind gifts from Marco Conti at University of California at San Francisco), Tnl (troponin I; 4002, Cell Signaling, Danvers, MA), phospho-Tnl at Ser23/24 (pTnlS23/24, 4004, Cell Signaling, Danvers, MA), and  $\gamma$ -tubulin (T6557, Sigma-Aldrich, St Louis, MO). The antibodies for  $\beta_1$ AR and LTCC have been validated previously.<sup>3,29</sup> IRDye 680RD goat anti-rabbit IgG secondary antibody (926–68071, LI-COR, Lincoln, NE) and IRDye 800CW goat anti-mouse IgG secondary antibody (926–32210, LI-COR, Lincoln, NE) were used for multicolor detection. PVDF membranes were scanned on Biorad Chemidoc MP imaging system (Biorad Laboratory, CA). The optical density of the bands was analyzed with National Institutes of Health Image J software (<https://imagej.nih.gov/ij/>).

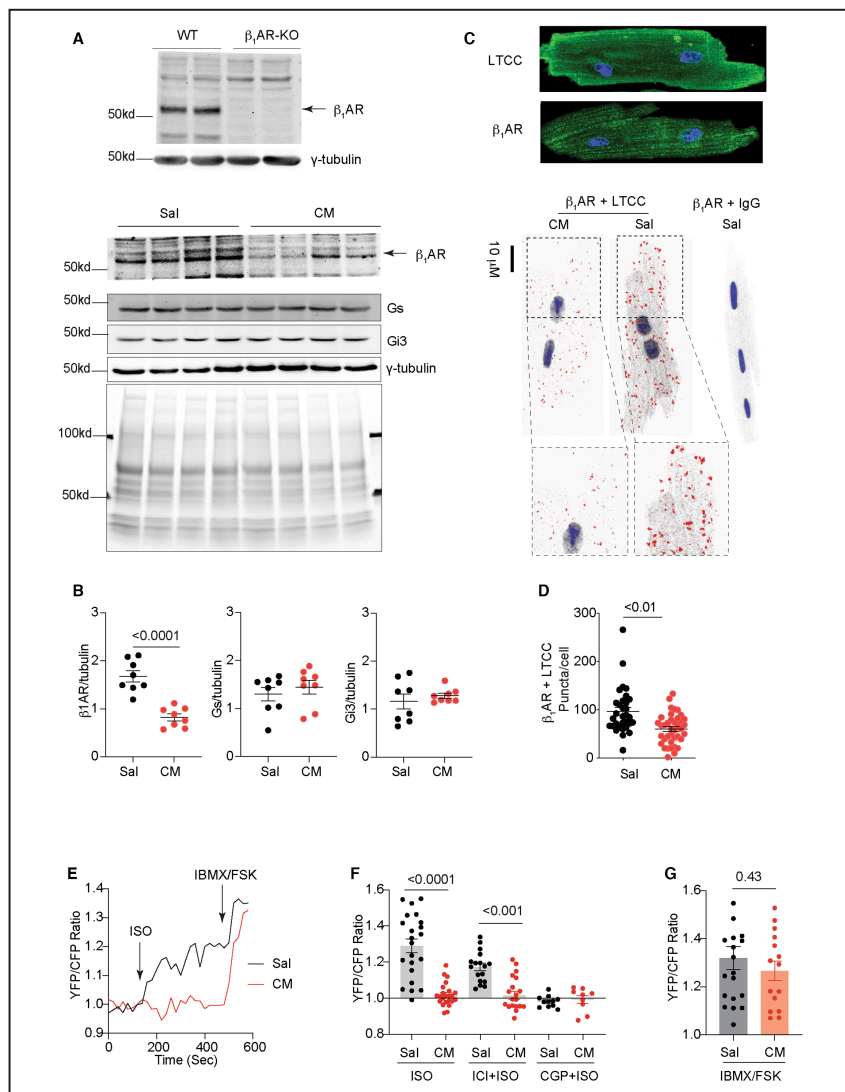


**Figure 1. Chronic adrenergic stress promotes the downregulation of cardiac  $\beta_1$ AR protein and signaling at the plasma membrane.**

**A and B**, Western blots show the specific detection of  $\beta_1$ AR in heart lysates from WT and  $\beta_1$ AR-KO mice, and protein levels of  $\beta_1$ AR, Gs, and Gi3 in the hearts after chronic infusion with saline and isoproterenol (cardiomyopathy) for 2 weeks. Multiple bands of  $\beta_1$ AR detected with antibody may be due to posttranslational modification of the receptor.<sup>33</sup> Coomassie blue staining shows total protein loads. N=8. *P* values were analyzed using Student's *t* test. **C and D**, Immunofluorescence staining of  $\beta_1$ AR and LTCC in AVMs. Proximity ligation assay to probe the association between  $\beta_1$ AR and LTCC on the plasma membrane in AVMs isolated from mice after chronic infusion with saline or isoproterenol. Dot plots representing mean $\pm$ SEM of the indicated number of AVMs from 5 mice. *P* values were analyzed using Student's *t* test. **E and F**, Time courses and maximal increases in PM-AKAR3 YFP/CFP ratio in AVMs after isoproterenol (100 nmol/L) stimulation alone or in the presence of  $\beta_1$ AR antagonist CGP20712a (CGP, 300 nmol/L) or  $\beta_2$ AR antagonist ICI118551 (ICI, 100 nmol/L). Isobutylmethylxanthine (100  $\mu$ mol/L) and forskolin (10  $\mu$ mol/L) were added after isoproterenol stimulation. *P* values were analyzed using 2-way ANOVA followed by Tukey's test. **G**, Maximal increases in YFP/CFP ratio of PM-AKAR3 after stimulation with isoproterenol or isobutylmethylxanthine+forskolin. Dot plots representing mean $\pm$ SEM of the indicated number of AVMs from 6 mice. *P* values were analyzed using Student's *t* test. AVM indicates adult ventricular myocyte;  $\beta_1$ AR,  $\beta_1$  adrenergic receptor; CFP, cyan fluorescent protein; CGP, CGP20712a; CM, cardiomyopathy; FSK, forskolin; Gs, stimulatory G protein, Gi3, inhibitory G protein 3; IBMX, isobutylmethylxanthine; ICI, ICI118551; ISO, isoproterenol; KO, knockout; LTCC, L-type calcium channel; PM-AKAR3, plasma membrane anchored a kinase activity reporter 3, Sal, saline; WT, wild type; and YFP, yellow fluorescent protein.



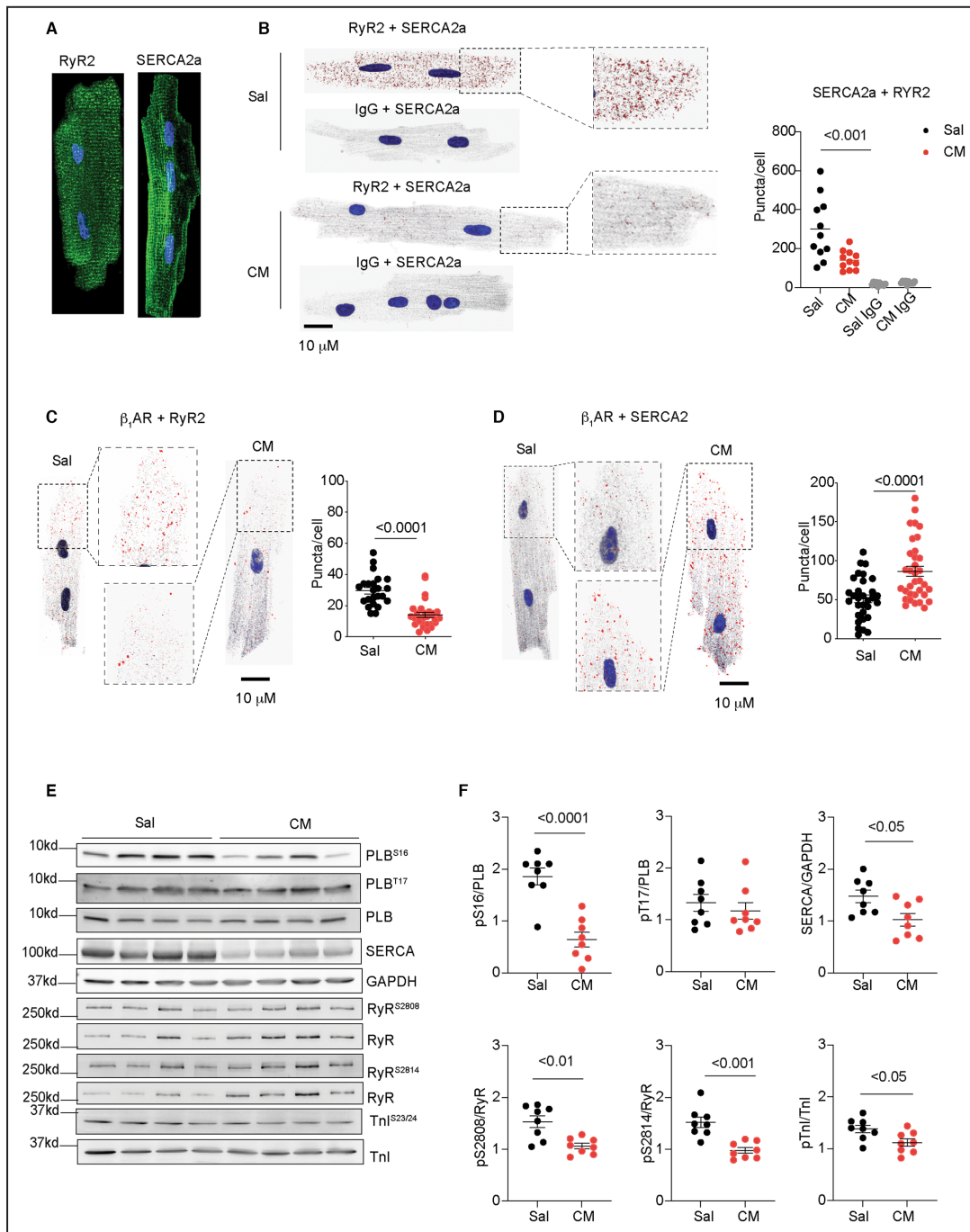


**Figure 2. Chronic adrenergic stress decreases  $\beta_1$ AR association with RyR2 and increases  $\beta_1$ AR association with SERCA2a.**

**A**, Immunofluorescence staining of RyR2 and SERCA2a in AVMs. **B**, Proximity ligation assay to probe the association between RyR2 and SERCA2a in AVMs isolated from mice after chronic infusion with saline or isoproterenol (CM). Dot plots represent mean±SEM of individual AVMs from 5 mice. *P* values were analyzed using 2-way ANOVA followed by Tukey's test. **C** and **D**, Proximity ligation assay to probe the association of  $\beta_1$ AR with RyR2 and SERCA2a in AVMs isolated from mice after chronic infusion with saline or isoproterenol. Dot plots represent mean±SEM of individual AVMs from 5 mice. *P* values were analyzed using Student's *t* test. **E** and **F**, The phosphorylation of PLB at serine 16 and threonine 17, RyR2 at serine 2808 and 2814, TnI at serine 23/24, and the total protein of PLB, SERCA2a, RyR2, and TnI were examined in Western blots and quantified in dot plots. N=8. Dot plots representing mean±SEM. *P* values were analyzed using Student's *t* test. AVM indicates adult ventricular myocyte;  $\beta_1$ AR,  $\beta_1$  adrenergic receptor; CM, cardiomyopathy; PLB, phospholamban; RyR2, ryanodine receptor 2; Sal, saline; SERCA2a, (Sarco)endoplasmic reticulum calcium ATPase 2a; and TnI, troponin I.

## Fluorescence Resonance Energy Transfer Assay

The FRET assay was carried out following the method reported before.<sup>22,23,27,28</sup> Briefly, AVMs were cultured in serum-free M1018 media with 6.25  $\mu$ mol/L blebbistatin (PH 7.35, Sigma-Aldrich). Cells were infected with adenoviruses expressing PM-AKAR3, FKBP-AKAR3, and SR-AKAR3<sup>22,23</sup> biosensors for 36 hours before recording (DMI3000 B, Buffalo Grove, IL). Recombinant adenoviruses were generated with the pAdeasy system (Qbiogene, Carlsbad, CA) as previously described.<sup>22,23,27,28</sup> The myocytes were recorded using Metafluor software (Molecular Devices, Sunnyvale, CA). CFP (cyan fluorescent protein) and YFP (yellow fluorescent protein) were imaged (200 milliseconds) with 20-second interval. AVMs were recorded at the baseline and after treatment with isoproterenol (100 nmol/L), ICI 118551 (ICI, I127, Sigma-Aldrich), CGP 20712a (CGP, C125, Sigma-Aldrich), rolipram (Sigma-Aldrich), isobutylmethylxanthine (HY-12318, MedChemExpress LLC), and forskolin (F-9929, LC Laboratories). Fluorescence emission intensity at 545 nm/L (YFP) and 480 nm/L (CFP) was subjected to background subtraction. YFP/CFP ratio was analyzed as F/F<sub>0</sub>, in which F is at time t and F<sub>0</sub> is the baseline. An increase in the YFP/CFP indicates the activation of PKA. The numbers of animals and cells were labeled in the figures.

## AVMs Sarcomere Shortening and Calcium Transient Detection

As previously reported,<sup>3,25,30</sup> freshly isolated AVMs were loaded with 5  $\mu$ mol/L Fluo-4 AM (Thermo Fisher Scientific, Waltham, MA) for 15 minutes in the dark at room temperature and rinsed with PBS without calcium for 10 minutes. AVMs were then placed on a dish and paced at 1 Hz with a SD9 stimulator (Grass Technology, Warwick, RI).

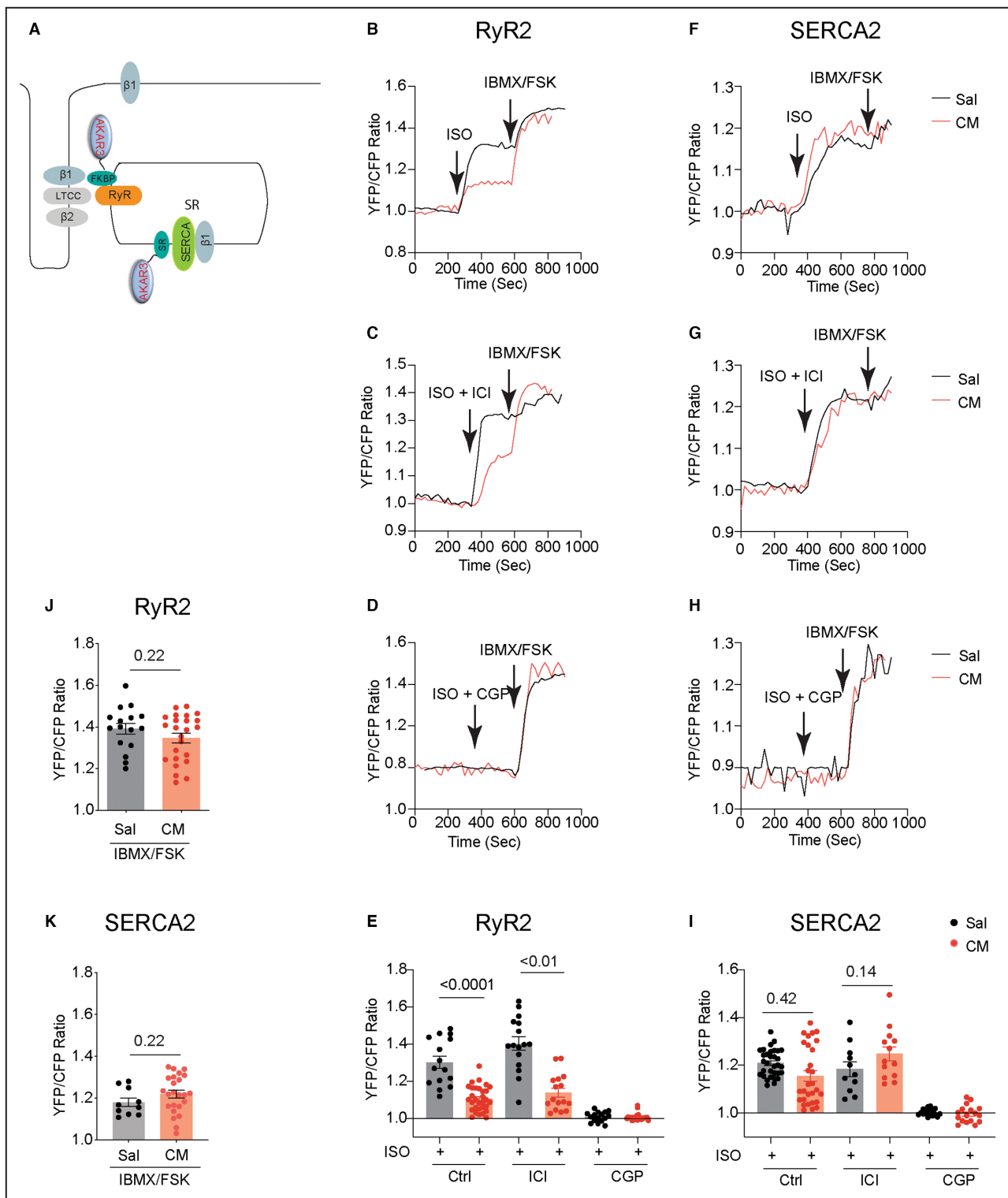
Metamorph software was used to image beating cells in a bright field or in 488 nm emission channel before and 5 minutes after drug administration with a Zeiss AX10 inverted fluorescence microscope (Zeiss AX10, Dublin, CA). Fractional shortening was analyzed in movies acquired in bright field using Metamorph software and calcium transient amplitude and decay time (Tau) were analyzed in movies acquired in 488 nm channel using customized software (Gailab) as reported.<sup>3,25,30</sup> The numbers of animals and cells were labeled in the figures.

## Proximity Ligation Assay

AVMs were fixed with 4% paraformaldehyde for 15 minutes. AVMs were permeabilized (0.2% NP-40, 2% goat serum in PBS) and incubated at 4 °C overnight with primary antibodies against  $\beta_1$ AR and LTCC Cav1.2,  $\beta_1$ AR and RyR2,  $\beta_1$ AR and SERCA2a, or RyR2 and SERCA2a (Table S1). Mouse normal IgG (sc-2025, Santa Cruz) were used as controls. SERCA2a (MAB2636, Millipore, CA), LTCC Cav1.2 (NeuroMab Clone N263/31), RyR2 (MA3-925, Thermo fisher, MA), and rabbit polyclonal  $\beta_1$ AR (sc-568, Santa Cruz, Dallas, TX) antibodies were used to detect the in situ interaction between  $\beta_1$ AR and LTCC, SERCA2a, or RyR in AVMs from isoproterenol infusion mice and the controls. After incubation with the primary antibodies, the AVMs were incubated with secondary antibodies against mouse and rabbit primary antibodies labeled with oligonucleotides, which when present within 40 nm undertake rolling circle amplification to generate a specific fluorescent signal after the addition of labeled probes. The samples were subjected to proximity ligation assay based on the manufacturer's protocol (Sigma-Aldrich). The color images of polymerized DNA were collected on a Leica Falcon SP8 confocal microscope and analyzed double-blindly on ImageJ. Representative figures/images reflected the average levels of each experiment.

### Figure 3. Chronic adrenergic stress selectively downregulates the $\beta_1$ AR-induced PKA activity at the RyR2 but not at the SERCA2a.

**A**, Cartoon illustrates the FKBP-AKAR3 and SR-AKAR3 biosensors to detect local PKA activities at the RyR2- and SERCA2a-associated nanodomains in AVMs. Mice were subjected to chronic infusion with saline or isoproterenol (CM). AVMs were isolated to express FKBP-AKAR3 or SR-AKAR3 biosensors. **B** through **D**, Time courses of FKBP-AKAR3 YFP/CFP ratio in AVMs after isoproterenol (100 nmol/L) stimulation and in the presence of  $\beta_1$ AR antagonist CGP20712a (CGP, 300 nmol/L) or  $\beta_2$ AR antagonist ICI118551 (ICI, 100 nmol/L). After isoproterenol stimulation, Isobutylmethylxanthine (100  $\mu$ mol/L) and forskolin (10  $\mu$ mol/L) were added. **E**, Data show maximal increases in YFP/CFP ratio of FKBP-AKAR3 after stimulation with isoproterenol alone or in the presence of  $\beta_1$ AR antagonist CGP (300 nmol/L) or  $\beta_2$ AR antagonist ICI (100 nmol/L). *P* values were analyzed using 2-way ANOVA followed by Tukey's test. **F** through **H**, Time courses of SR-AKAR3 YFP/CFP ratio in AVMs after stimulation with isoproterenol (100 nmol/L) and in the presence of  $\beta_1$ AR antagonist CGP or  $\beta_2$ AR antagonist ICI. Isobutylmethylxanthine (100  $\mu$ mol/L) and forskolin (10  $\mu$ mol/L) were added after isoproterenol stimulation. **I**, Data show maximal increases in YFP/CFP ratio of SR-AKAR3 after stimulation with isoproterenol alone or in the presence of  $\beta_1$ AR antagonist CGP (300 nmol/L) or  $\beta_2$ AR antagonist ICI (100 nmol/L). *P* values were analyzed using 2-way ANOVA followed by Tukey's test. **J** and **K**, Data show maximal increase in YFP/CFP ratio of SR-AKAR3 and FKBP-AKAR3 after stimulation with isobutylmethylxanthine and forskolin. Dot plots representing mean  $\pm$  SEM of the indicated number of AVMs from 5 Sal and 8 CM mice. *P* values were analyzed using Student's *t* test. AVM indicates adult ventricular myocyte;  $\beta_1$ AR,  $\beta_1$  adrenergic receptor; CFP, cyan fluorescent protein; CGP, CGP20712a; CM, cardiomyopathy; FKBP-AKAR3, FK506 binding protein 12.6 anchored a kinase activity reporter 3; FSK, forskolin; IBMX, isobutylmethylxanthine; ICI, ICI118551; ISO, isoproterenol; PKA, protein kinase A; RyR2, ryanodine receptor 2; Sal, saline; SERCA2a, (Sarco)endoplasmic reticulum calcium ATPase 2a; SR-AKAR3, sarcoplasmic reticulum anchored a kinase activity reporter 3; and YFP, yellow fluorescent protein.



**Statistical Analysis**

All data are expressed as mean $\pm$ SEM. The sample size was calculated using power analysis with a power of 0.8 for a value of  $\alpha=0.05$ . To achieve statistical significance, the sample size (number) was at least 5. An unpaired, 2-tailed Student *t* test was used for 2-group

comparisons and ANOVA with multiple testing correction for 3 or more group comparisons, performed on continuous, normally distributed data assessed in GraphPad Prism 9 with significance at  $\alpha=0.05$  (GraphPad Inc., San Diego, CA).  $P\leq 0.05$  was considered significant.

## RESULTS

### Chronic Adrenergic Stress Promotes the Downregulation of $\beta_1$ AR and Signaling at the PM and RyR2 Complexes

We examined the alteration of adrenergic signaling in cardiomyopathy induced by chronic isoproterenol infusion (60 mg/kg per day, 2 weeks). The isoproterenol infusion-induced cardiomyopathy was featured with decreased ejection fraction (Table S2).<sup>5,31,32</sup> After chronic isoproterenol infusion, mouse hearts displayed reduced protein level of the  $\beta_1$ AR but not G proteins (Figure 1A and 1B<sup>33</sup>). We performed proximity ligation assay between  $\beta_1$ AR and LTCC to examine the receptor association with LTCC on the PM of AVMs isolated from mice after saline and isoproterenol infusion. AVMs from the isoproterenol-infused hearts displayed a reduced  $\beta_1$ AR association with LTCC compared with saline controls (Figure 1C and 1D). We also applied FRET-based PKA biosensor AKAR3 anchored on the PM (PM-AKAR3) to detect PKA activity induced by adrenergic stimulation (Figure 1E). In AVMs from saline-infused mice, stimulation with isoproterenol induced robust increases in the FRET ratio of PM-AKAR3 biosensor, indicating increases in PKA activities (Figure 1E).  $\beta_1$ AR blocker CGP20712a but not  $\beta_2$ AR blocker ICI118551 abolished the adrenergic-induced PKA activities at the PM in AVMs (Figure 1F). However, isoproterenol minimally increased the FRET ratio of PM-AKAR3 biosensors in AVMs from mice after chronic isoproterenol infusion (Figure 1E and 1F). As a control, isobutylmethylxanthine and forskolin promoted equivalent PKA activities in AVMs from both saline and isoproterenol-infused mice (Figure 1E and 1G). These data suggest cardiac  $\beta_1$ AR-PKA signaling is downregulated at the PM in AVMs after chronic adrenergic stress. Both SERCA2a and RyR2 are distributed on the SR membrane. SERCA2a and RyR2 also displayed an association in healthy AVMs, which was drastically reduced in AVMs from the isoproterenol-infused mice (Figure 2A and 2B). We have recently shown that an intracellular pool of  $\beta_1$ AR selectively forms complexes

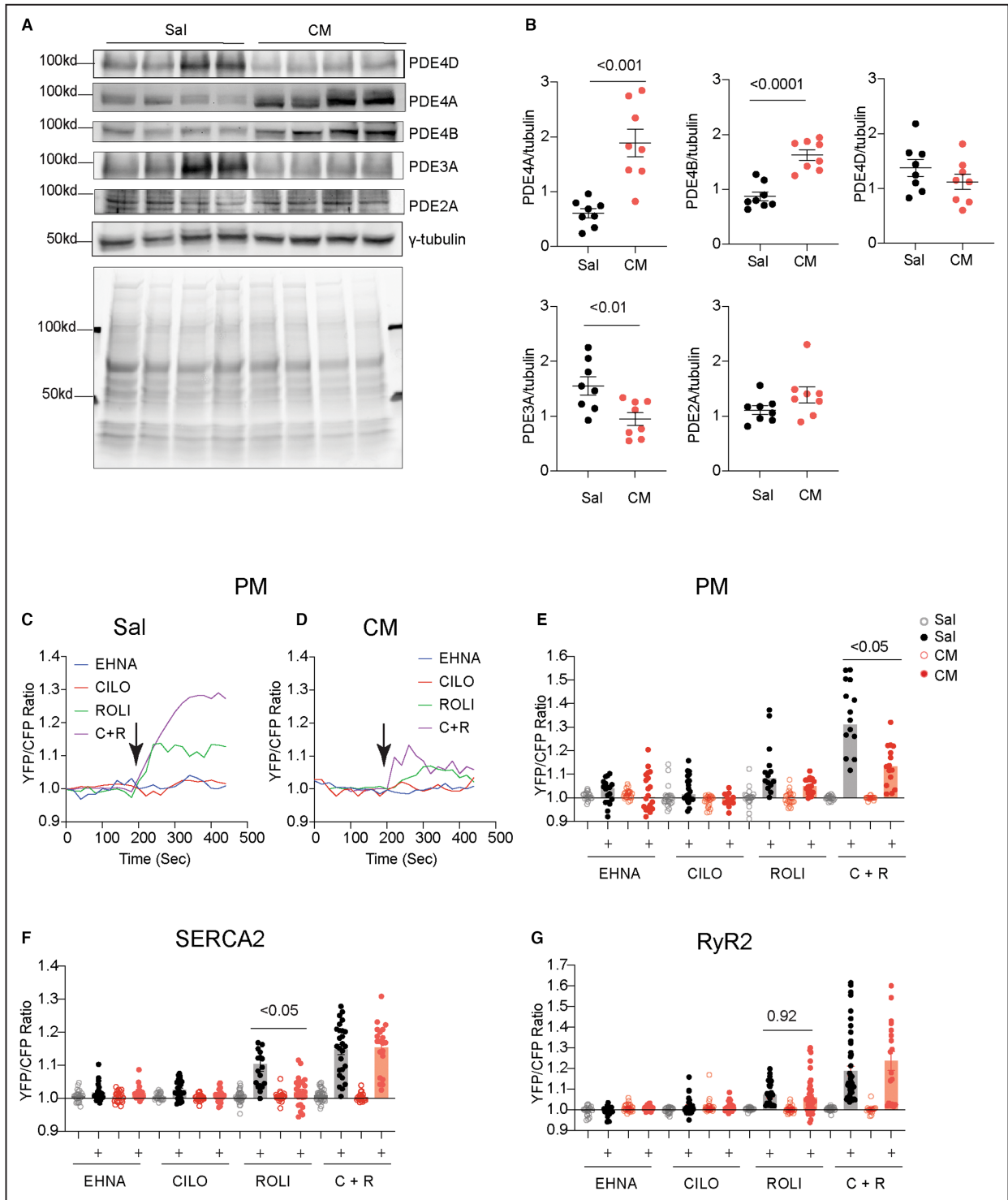
with SERCA2a,<sup>4,5</sup> which draws a contrast to the receptor at the PM. In isolated AVMs, we examined the  $\beta_1$ AR association with RyR2 and SERCA2a at the SR. The isoproterenol-infused mice displayed reduced  $\beta_1$ AR association with RyR2 in AVMs (Figure 2C), whereas the association of  $\beta_1$ AR with SERCA2a was increased (Figure 2D). Meanwhile, the isoproterenol-infused hearts displayed reduced phosphorylation of RyR2 at serine 2808 and 2814 relative to saline controls (Figure 2E through 2F). The PKA phosphorylation of PLB at serine 16 was also reduced in the isoproterenol-infused hearts, together with reduced SERCA2a protein expression (Figure 2E through 2F). Additionally, the hearts displayed minimal changes in phosphorylation of PLB at the  $\text{Ca}^{2+}$ /calmodulin-dependent protein kinase II site of threonine 17 and phosphorylation of Tnl at serine 23/24 after isoproterenol infusion relative to saline groups (Figure 2E through 2F).

When we applied PKA biosensor FKBP-AKAR3 anchored to RyR2<sup>24</sup> and SR-AKAR3 anchored to SERCA2a<sup>22,23</sup> to analyze the subcellular  $\beta_1$ AR-PKA signaling in AVMs (Figure 3A). AVMs from the isoproterenol-infused mice displayed a lower adrenergic-induced PKA activity at the RyR2 than saline controls (Figure 3B through 3E). The adrenergic-induced PKA activities at the RyR2 were abolished by  $\beta_1$ AR blocker CGP20712a but not  $\beta_2$ AR blocker ICI118551 in AVMs from both saline and isoproterenol-infused hearts (Figure 3C through 3E). In comparison, AVMs from saline and isoproterenol-infused hearts displayed similar adrenergic-PKA signaling at the SERCA2a, which was blocked by CGP20712a but not by ICI118551 (Figure 3F through 3I). These data indicate that the isoproterenol-induced  $\beta_1$ AR signaling is selectively desensitized at the RyR2 in AVMs from the isoproterenol-infused mice. Meanwhile, isobutylmethylxanthine and forskolin promoted equivalent PKA activities at RyR2 and SERCA2a between AVMs from saline and isoproterenol-infused mice, respectively (Figure 3J and 3K). These data suggest distinct remodeling of  $\beta_1$ AR-PKA signaling at the RyR2 and SERCA2a complexes in the hearts after chronic adrenergic stimulation.

#### Figure 4. Chronic adrenergic stress changes the protein expression levels of phosphodiesterase isoforms and subcellular PKA activities at the RyR2 and SERCA2a.

**A and B**, Western blots show the protein levels of PDE2A, PDE3A, PDE4A, PDE4B, and PDE4D in the hearts after chronic infusion of saline or isoproterenol (CM). Coomassie blue staining shows total protein loads. N=8. Data represent mean $\pm$ SEM of individual mice. *P* values were obtained using Student's *t* test. **C and D**, Time courses show PM-AKAR3 YFP/CFP ratio after treatment with PDE2 inhibitor EHNA (10  $\mu$ mol/L), PDE3 inhibitor cilostamide (1  $\mu$ mol/L), PDE4 inhibitor rolipram (10  $\mu$ mol/L), or the combination of PDE3 and PDE4 inhibitor in AVMs from Sal and isoproterenol-infused hearts. **E through G**, The baseline and maximal YFP/CFP ratio of PM-AKAR3, SR-AKAR3, and FKBP-AKAR3 after treatment with PDE inhibitors. Dot plots represent mean $\pm$ SEM of individual AVMs. *P* values were analyzed using 2-way ANOVA followed by Tukey's test. AVM indicates adult ventricular myocyte; C+R, cilostamide+rolipram; CFP, cyan fluorescent protein; Cilo, cilostamide; CM, cardiomyopathy; EHNA, erythro-9-(2-hydroxy-3-nonyl)adenine; FKBP-AKAR3, FK506 binding protein 12.6 anchored a kinase activity reporter 3; PDE2A, phosphodiesterase 2A; PDE3A, phosphodiesterase 3A; PDE4D, phosphodiesterase 4D; PDE4A, phosphodiesterase 4A; PDE4B, phosphodiesterase 4B; PKA, protein kinase A; PM-AKAR3, plasma membrane anchored a kinase activity reporter 3; RyR2, ryanodine receptor 2; Sal, saline; SERCA2a, (Sarco)endoplasmic reticulum calcium ATPase 2a; SR-AKAR3, sarcoplasmic reticulum anchored a kinase activity reporter 3; Roli, rolipram; and YFP, yellow fluorescent protein.





**Chronic Adrenergic Stress Alters the Protein Levels of PDE3 and 4 Isoforms to Affect the Local PKA Activity at the RyR2 Complexes**

We have previously shown that PDE4D isoforms associate with cardiac  $\beta_1$ AR and  $\beta_2$ AR and regulate subcellular cAMP-PKA activity in AVMs.<sup>13-15</sup> Cardiac diseases

are associated with altered PDE gene expression in the myocardium.<sup>25</sup> Among the highly expressed cardiac PDEs, we showed that cardiac PDE3A were reduced in the hearts after chronic isoproterenol infusion (Figure 4A and 4B). In comparison, PDE4A and PDE4B displayed increased protein levels in the isoproterenol-infused hearts (Figure 4A and 4B). We assessed the individual PDE genes in controlling local cAMP-PKA

activities at different subcellular membranes. Inhibiting PDE4, but not PDE2 and PDE3, increased PKA activity at the PM in the control AVMs from saline mice (Figure 4C through 4E). Inhibition of PDE4 and PDE3 also synergistically enhanced PKA activities at the PM in control AVMs (Figure 4C through 4E). In AVMs from the mice after chronic isoproterenol infusion, inhibition of PDE4 alone or PDE3 and PDE4 together yielded smaller increases in PKA activities at the PM than saline controls (Figure 4D and 4E). Meanwhile, inhibition of PDE4 but not PDE2 and PDE3 promoted increases in PKA activities at the RyR2 and SERCA2a complexes in the control AVMs from saline mice (Figure 4F and 4G). Inhibition of PDE3 and PDE4 synergistically increased PKA activities at the RyR2 and SERCA2a complexes (Figure 4F and 4G). In AVMs from the mice after chronic isoproterenol infusion, the PDE4 inhibitor-induced response was attenuated at the SERCA2a but not in the RyR2 complexes (Figure 4F and 4G).

### Inhibition of PDE3 and 4 Selectively Modulates the $\beta_1$ AR Signaling at the RyR2 Complexes

PDE4D isoforms are functionally linked to cardiac  $\beta_1$ AR and  $\beta_2$ AR signaling in AVMs.<sup>13–16</sup> We further assessed the impacts of PDE4 inhibitors on adrenergic stimulation of local PKA activities in AVMs from mice after chronic saline or isoproterenol infusion. Inhibiting PDE4 did not alter the adrenergic stimulation of PKA activity at the PM and SERCA2a and RyR2 complexes in AVMs from saline control mice (Figure 5A through 5F). In AVMs from mice with chronic isoproterenol infusion, inhibiting PDE4 enhanced adrenergic stimulation of PKA activity at the PM but did not change the responses at the SERCA2a and RyR2 complexes (Figure 5G through 5I). Recent studies indicate that PDE2 and PDE3 may have increased roles in regulating cardiac adrenergic signaling in hypertrophic hearts.<sup>28,34</sup> Inhibiting either PDE2 or PDE3 enhanced adrenergic stimulation of PKA activities

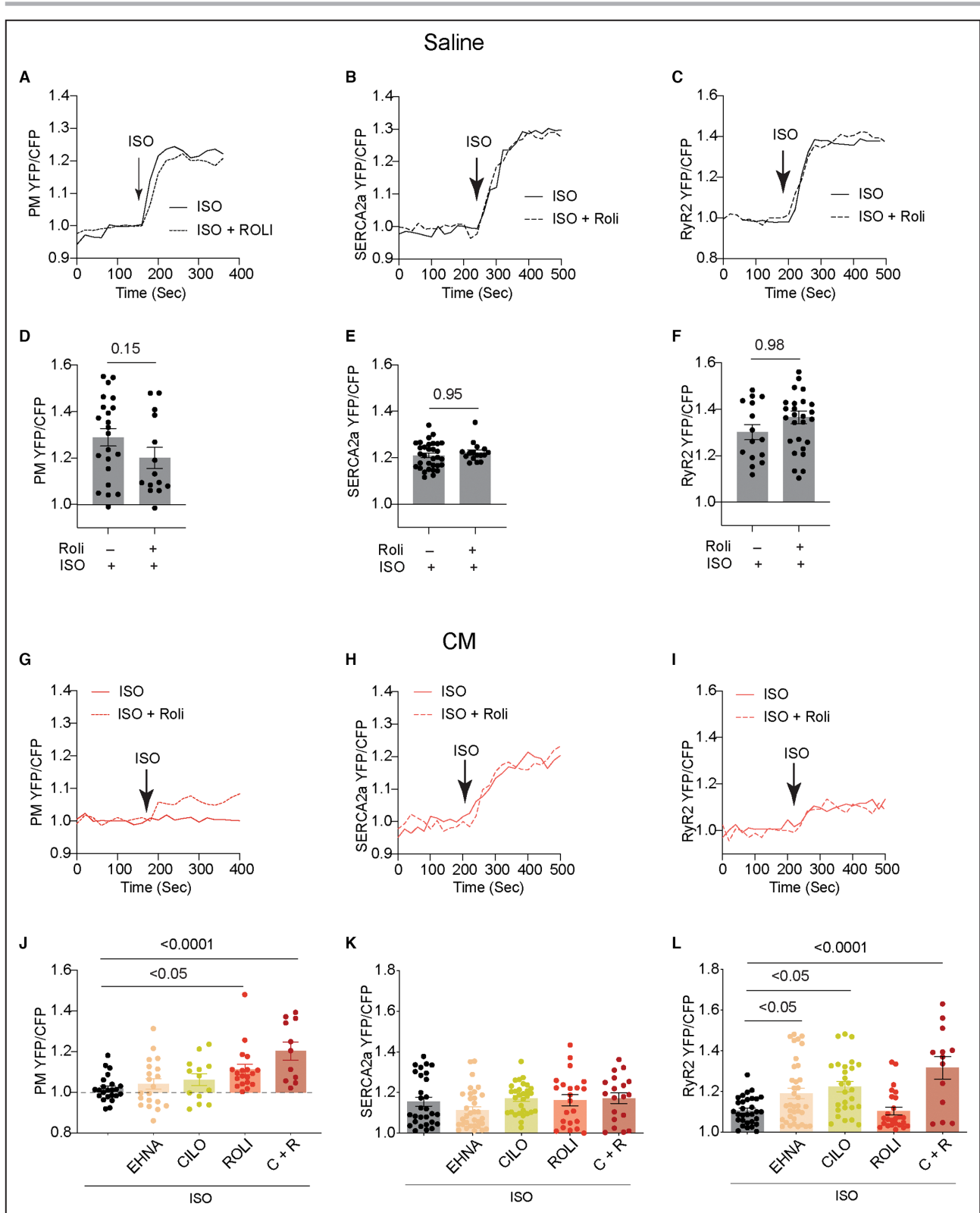
at the RyR2 complexes but not the PM and SERCA2a complexes in the AVMs from isoproterenol-infused hearts (Figure 5J through 5L). Additionally, dual inhibition of PDE3 and PDE4 enhanced the adrenergic stimulation of PKA activities at the PM and RyR2 complexes but not the SERCA2a complexes in the hearts after chronic isoproterenol infusion (Figure 5J through 5L). Inhibiting PDE4 also enhanced adrenergic stimulation of calcium transient amplitude and sarcomere contractile shortening in AVMs from saline control mice (Figure 6A through 6E). Although the adrenergic responses were reduced in AVMs from mice after chronic isoproterenol infusion, the effects of the PDE4 inhibitor were detected in calcium transient tau but not amplitude and sarcomere shortening (Figure 6A through 6E). Interestingly, inhibiting PDE3 rescued adrenergic responses in calcium transient amplitude and sarcomere contractile shortening, whereas inhibiting PDE2 only restored the isoproterenol-induced calcium transient amplitude (Figure 6F through 6J). Addition of isobutylmethylxanthine and forskolin induced similar increases in calcium cycling and sarcomere shortening in AVMs from the saline and isoproterenol-infused mice (Figure 6K through 6M). These data suggest that inhibition of PDE3 is an effective strategy to restore PKA activity at the RyR2, calcium cycling, and contractile shortening in AVMs from the mice after chronic isoproterenol infusion.

### Inhibition of Monoamine Oxidase Rescues the $\beta_1$ AR-Induced PKA Activity at the SERCA2a Complexes in Cardiomyopathy

Catecholamine-induced PKA activity at the SERCA2a is subjected to additional regulation by catecholamine transport and metabolism in AVMs.<sup>4–6</sup> MAO-A (monoamine oxidase A) is upregulated in HF to increase catecholamine metabolism.<sup>35,36</sup> We found that the endogenous norepinephrine induced a smaller increase in PKA activity at the SERCA2a and RyR2 in AVMs

#### Figure 5. Inhibiting PDE affects the isoproterenol-induced subcellular PKA activities in AVMs from mice after chronic infusion with isoproterenol.

Mice were subjected to chronic infusion with saline or isoproterenol. AVMs were isolated to express PM-AKAR3, FKBP-AKAR3, and SR-AKAR3 biosensors. **A** through **C**, AVMs from saline-infused mice were stimulated with isoproterenol (100 nmol/L) alone or together with PDE4 inhibitor rolipram (10  $\mu$ mol/L). Time courses show PM-AKAR3, SR-AKAR3, and FKBP-AKAR3 YFP/CFP ratio in AVMs after treatment. **D** through **F**, Dot plots represent mean  $\pm$  SEM of YFP/CFP ratio in individual AVMs from 5 mice. *P* values were analyzed using Student's *t* test. **G** through **I**, AVMs from isoproterenol-infused mice were stimulated with isoproterenol (100 nmol/L) alone or together with PDE4 inhibitor rolipram (10  $\mu$ mol/L). Time courses show PM-AKAR3, SR-AKAR3, and FKBP-AKAR3 YFP/CFP ratio in AVMs after treatment with isoproterenol and rolipram. **J** through **L**, AVMs from isoproterenol-infused mice were stimulated with isoproterenol (100 nmol/L) alone or together with PDE2 inhibitor EHNA (10  $\mu$ mol/L), PDE3 inhibitor cilostamide (1  $\mu$ mol/L), PDE4 inhibitor rolipram (10  $\mu$ mol/L), or the combination of cilostamide and rolipram. Dot plots representing mean  $\pm$  SEM of YFP/CFP ratio in individual AVMs from 5 mice. *P* values were analyzed using 1-way ANOVA followed by Tukey's test. AVM indicates adult ventricular myocyte; C+R, cilostamide+rolipram; CFP, cyan fluorescent protein; Cilo, cilostamide; CM, cardiomyopathy; EHNA, erythro-9-(2-hydroxy-3-nonyl) adenine; FKBP-AKAR3, FK506 binding protein 12.6 anchored a kinase activity reporter 3; ISO, isoproterenol; PDE, phosphodiesterase; PKA, protein kinase A; PM-AKAR3, plasma membrane anchored a kinase activity reporter 3; Roli, rolipram; RyR2, ryanodine receptor 2; Sal, saline; SERCA2a, (Sarco)endoplasmic reticulum calcium ATPase 2a; SR-AKAR3, sarcoplasmic reticulum anchored a kinase activity reporter 3; and YFP, yellow fluorescent protein.



from the isoproterenol-infused mice relative to saline controls, respectively (Figure 7A and 7B). Inhibition of MAO-A selectively rescued the norepinephrine-induced response at the SERCA2a but not the RyR2 (Figure 7A and 7B). Accordingly, norepinephrine induced smaller

responses in calcium cycling and sarcomere contractile shortening in AVMs from the isoproterenol-infused mice relative to saline controls (Figure 7C through 7G); inhibiting MAO-A restored the norepinephrine-induced calcium cycling and sarcomere contractile shortening

(Figure 7C through 7G). These data suggest that the catecholamine-induced internal  $\beta_1$ AR activity at the SERCA2a is suppressed by MAO-A-mediated metabolism in AVMs from the isoproterenol-infused mice.

## DISCUSSION

In this study, we have characterized distinct mechanisms for the downregulation of subcellular adrenergic signaling at the PM and RyR2 and SERCA2a complexes in AVMs from the mice after chronic adrenergic stress. The  $\beta_1$ AR protein levels and association with LTCC and RyR2 were reduced in hearts after chronic isoproterenol infusion. The  $\beta_1$ AR-PKA signaling and PKA phosphorylation of substrates at these subcellular locations were reduced. Inhibition of PDE3 rescued the adrenergic-induced PKA activity at the RyR2 complexes and sarcomere contractile shortening in AVMs isolated from the isoproterenol-infused mice. In comparison, the  $\beta_1$ AR association with SERCA2a was increased even though the PKA phosphorylation of phospholamban in the hearts was reduced after chronic isoproterenol infusion. Further studies revealed a reduced endogenous catecholamine (norepinephrine)-induced PKA activity at the SERCA2a complexes. Inhibition of MAO-A rescued the norepinephrine-induced PKA activity at the SERCA2a complexes, calcium cycling, and sarcomere contractile shortening in AVMs from the mice after chronic isoproterenol infusion. Our data uncover distinct mechanisms underlying the downregulation of  $\beta_1$ AR signaling at subcellular membranes for cardiac contraction and relaxation and reveal strategies to restore the local PKA activity and cardiac excitation-contraction coupling in AVMs from the mice after chronic isoproterenol infusion (Figure 7H and 7I).

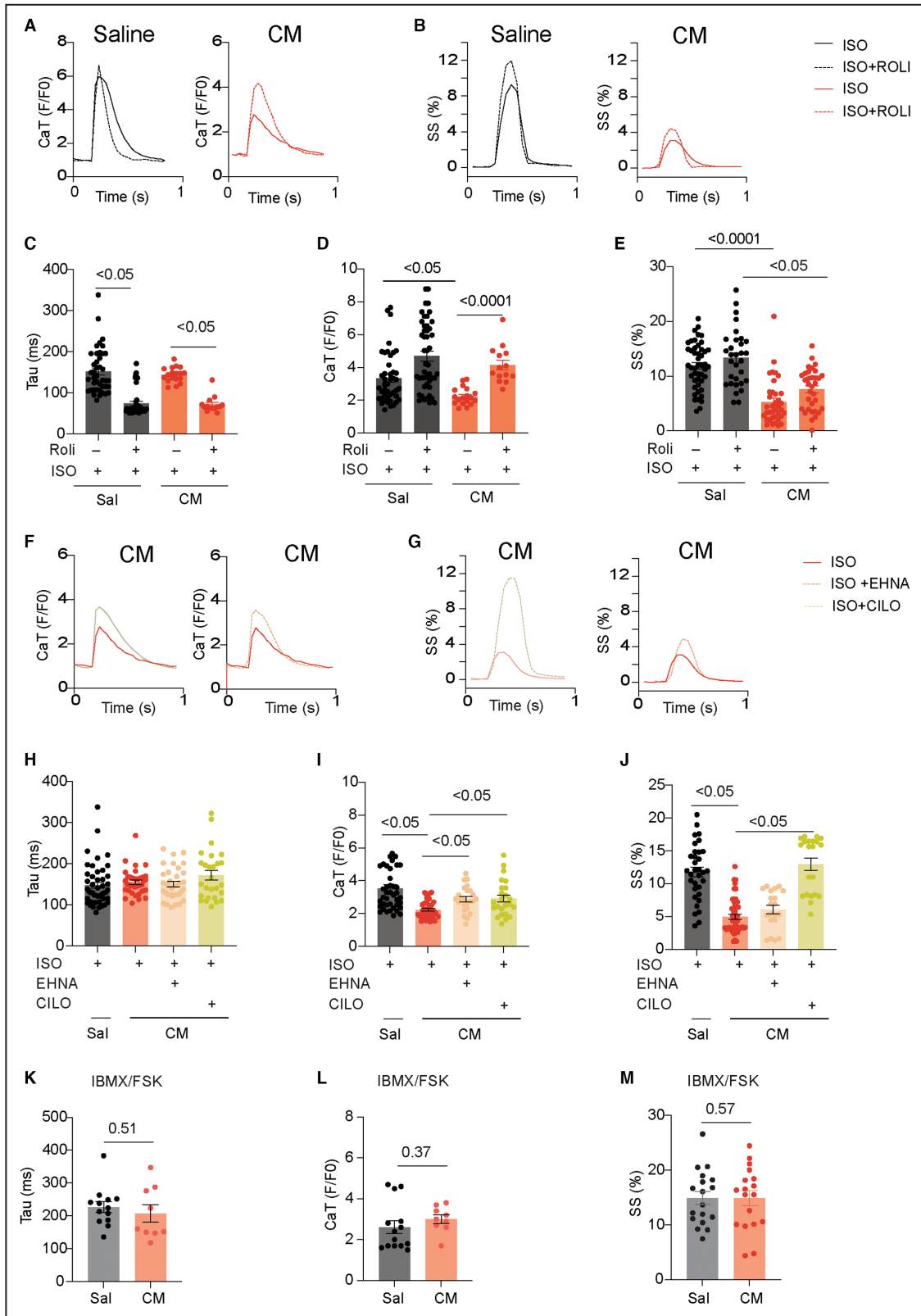
In AVMs, the RyR2- and SERCA2a-mediated SR calcium release and uptake critically affect myocyte calcium cycling, thus regulating cardiac systolic and diastolic function.<sup>7,8</sup>  $\beta$ -adrenergic signaling increases RyR2 and SERCA2a function by PKA-dependent

phosphorylation of RyR2 and PLB. Despite the elevated sympathetic drive in HF, a reduced PKA phosphorylation of PLB is often observed, leading to impaired SERCA2a function and calcium reuptake to the SR.<sup>6,37-39</sup> In comparison, RyR2 usually displays either minimal change or increased activity in HF, leading to increased SR calcium leakage.<sup>31,40,41</sup> The mechanisms underlying these alterations are not entirely understood. LTCC is tightly coupled to RyR2 at the junctional SR, reflecting the strong interaction between the 2 membranes.<sup>42</sup> Thus, a fraction of RyR2 interacts with LTCC at the junctional SR, forming a local functional unit likely controlled by the  $\beta_1$ AR in the vicinity. Previous studies show that cardiac  $\beta_1$ AR is not degraded but is redistributed from the PM to intracellular compartments via receptor endocytosis at an early stage of human HF.<sup>43</sup> Similarly,  $\beta_1$ AR does not display downregulation at the adaptive stage of HF development in a transverse aortic constriction model.<sup>34</sup> In this study, under chronic infusion with a high concentration of isoproterenol, the reduced  $\beta_1$ AR protein level is detected; thus, both the  $\beta_1$ AR protein level and distribution could contribute to the reduced receptor association with LTCC and RyR2. Accordingly, we detected reduced PKA activity at the PM and RyR2 complexes, likely in junctional SR. These observations are consistent with the downregulation of  $\beta_1$ AR signaling at the PM and RyR2 complexes in rabbit HF models and human HF with reduced ejection fraction.<sup>28,34</sup> Whereas others have observed a significant increase in  $\beta_2$ AR signaling to the RyR2 complexes in AVMs from a transaortic constriction mouse model and human HF with reduced ejection fraction,<sup>34</sup> we did not observe such changes in the model with chronic isoproterenol infusion. These data indicate that cardiac  $\beta$ AR signaling undergoes dynamic adaptations in a disease model- and stage-dependent manner, likely depending on the activity of the sympathetic drive and other factors such as mechanical stress and disease development. The impaired PKA signaling at the RyR2

### Figure 6. Inhibiting PDE rescues the adrenergic-induced subcellular PKA activity and E-C coupling in AVMs from mice after chronic infusion with isoproterenol.

AVMs from saline and isoproterenol (CM)-infused mice were loaded with fluo-4 dye and paced at 1 Hz. CaT decay tau and amplitude and SS were recorded in AVMs after stimulation with isoproterenol. **A** and **B**, AVMs were stimulated with isoproterenol (100 nmol/L) in the presence of PDE4 inhibitor rolipram (10  $\mu$ mol/L). CaT amplitude decay tau and SS were recorded in AVMs. Representative traces show CaT and SS. **C** through **E**, Data show maximal CaT amplitude and decay tau and SS in AVMs after stimulation. Dot plots representing mean  $\pm$  SEM of individual AVMs from 6 mice. *P* values were analyzed using 2-way ANOVA followed by Tukey's test. **F** through **G**, AVMs were stimulated with isoproterenol (100 nmol/L) in the presence of PDE2 inhibitor EHNA (10  $\mu$ mol/L) or PDE3 inhibitor cilostamide (1  $\mu$ mol/L) as indicated. Representative traces show CaT and SS. **H** through **J**, Data show maximal CaT amplitude and decay tau and SS in AVMs after stimulation. Dot plots representing mean  $\pm$  SEM of individual AVMs from 6 mice. *P* values were analyzed using 2-way ANOVA followed by Tukey's test. **K** through **M**, AVMs were stimulated with isobutylmethylxanthine (100  $\mu$ mol/L) and forskolin (10  $\mu$ mol/L). Data show maximal CaT amplitude and decay tau and SS in AVMs after stimulation. Dot plots representing mean  $\pm$  SEM of individual AVMs from 6 mice. *P* values were analyzed using Student's *t*-test. AVM indicates adult ventricular myocyte; CM, cardiomyopathy; CaT, calcium transient; Cilo, cilostamide; E-C, excitation-contraction; EHNA, erythro-9-(2-hydroxy-3-nonyl)adenine; FSK, forskolin; IBMX, isobutylmethylxanthine; ISO, isoproterenol; PDE, phosphodiesterase; PKA, protein kinase A; Roli, rolipram; Sal, saline; SS, sarcomere shortening; and tau, taurine.





complexes likely contributes to impaired ion channel function, calcium cycling, and cardiac contractility.

On the other hand, SERCA2 may be enriched in numerous endoplasmic reticulum/SR membrane

domains. Our proximity ligation assay shows an association of SERCA2a with RyR2, which may include the codistribution of both proteins within junctional SR. However, an internal pool of  $\beta_1$ AR associates with

SERCA2a on the SR but minimally associates with RyR2,<sup>4</sup> indicating that the internal  $\beta_1$ AR in association with SERCA2a likely forms a functional unit devoid of RyR2. Moreover, SERCA2a and RyR2 are regulated by different phosphatases and PDEs,<sup>17–21</sup> further supporting the presence of distinct signaling and functional units on the SR. Recent studies show that the SERCA2a-associated  $\beta_1$ AR is critical to regulating PLB phosphorylation, calcium reuptake, and cardiac diastolic relaxation.<sup>4,11</sup> Interestingly, we observed an increased association of  $\beta_1$ AR with SERCA2a with no reduction of  $\beta_1$ AR-PKA signaling to the SERCA2a complexes in AVMs from mice with chronic isoproterenol infusion. The increased association between  $\beta_1$ AR and SERCA2a may be due to altered protein expression and distribution of  $\beta_1$ AR in AVMs. For example, the  $\beta_1$ AR may be relocated to the SR after endocytosis; alternatively, the newly synthesized  $\beta_1$ AR may be functionally retained in the SR to support the local signaling at the SERCA2a nanodomains during the development of HF.<sup>5</sup> The mechanisms underlying the protein expression and distribution of  $\beta_1$ AR, RyR2, and SERCA2a remain to be explored in future studies.

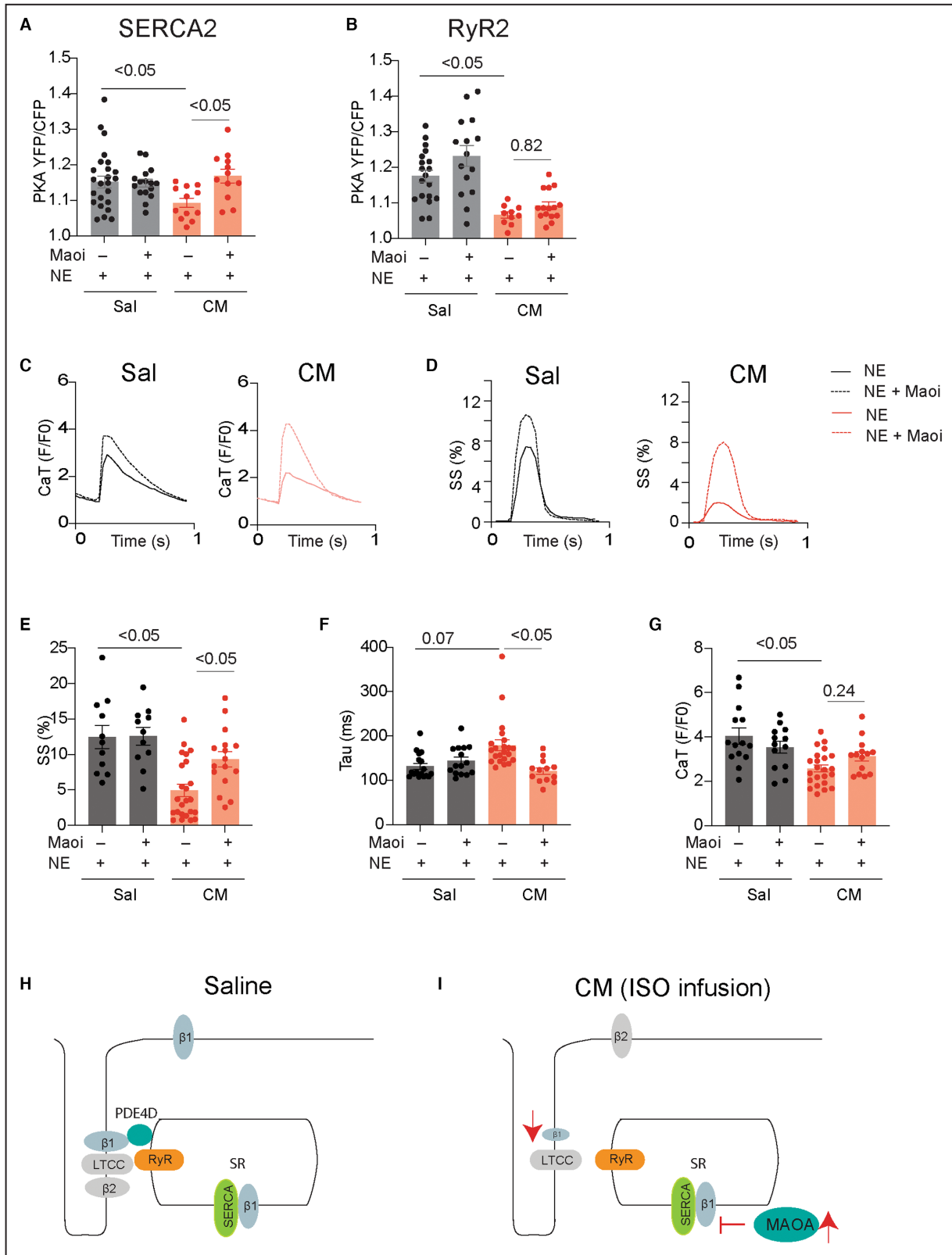
Even though the endogenous catecholamines are generally increased, HF still displays a downregulation of SERCA2a function associated with reduced PKA phosphorylation of PLB. The apparent contradictory observations are likely due to the increased expression of MAO-A in cardiac diseases,<sup>35,36</sup> which metabolizes the catecholamines and prevents them from accessing the internal pool of  $\beta_1$ AR at the SERCA2a-associated SR membrane nanodomains.<sup>4–6</sup> We show that inhibition of MAO-A selectively rescued the norepinephrine-induced local PKA activity at the SERCA2a but not at the RyR2 complexes. Inhibition of MAO-A partially rescued calcium cycling and sarcomere contractile shortening in AVMs from the isoproterenol-infused mice. In

comparison, isoproterenol is not a perfect MAO-A substrate, and the isoproterenol responses are not dependent on MAO-A. These data highlight the alternations of cardiac signaling for impaired cardiac relaxation in isoproterenol infusion-induced cardiomyopathy.

Among PDE genes expressed in mouse hearts, PDE4 and PDE3 are 2 families linked to the local cAMP and PKA activities at the RyR2 and SERCA2a complexes.<sup>17–21</sup> Here, we observed decreases in PDE3A and PDE4D and increases in PDE2A, PDE4A, and PDE4B protein levels. Previous studies also reveal dynamic alteration of PDE isoform activities in different membrane compartments in a rabbit HF model induced by combined aortic insufficiency and stenosis<sup>28</sup> and in a mouse HF model with transaortic constriction.<sup>34</sup> We observed that inhibition of PDE2 and PDE3 but not PDE4 enhanced the isoproterenol-induced PKA signaling at the RyR2 complexes. Moreover, inhibition of PDE3 also partially rescued calcium cycling and sarcomere shortening in AVMs from the isoproterenol-infused mice, supporting its clinical utility as an inotropic agent. Similarly, in mouse models with transaortic constriction, PDE2, and PDE3 display increased roles in controlling adrenergic signaling at the RyR2 complexes.<sup>34</sup> However, PDE3 inhibitors could potentially promote SR calcium leakage, arrhythmias, and detrimental effects by increasing RyR2 function.<sup>44</sup> Due to unfavorable outcomes of the long-term usage of these agents in patients, PDE3 inhibitors are limited only to acute human HF therapy.<sup>45</sup> Meanwhile, PDE4 had a diminished role in controlling adrenergic signaling at the RyR2 complexes in AVMs from the isoproterenol-infused mice, consistent with the reported dissociation between PDE4D3 and RyR2, leading to elevated PKA phosphorylation of RyR2 and calcium leakage in human HF.<sup>17,46</sup>

**Figure 7. Inhibition of MAO-A rescues the norepinephrine-induced PKA activity at the SERCA2a nanodomains and E-C coupling in AVMs from mice cardiomyopathy.**

**A and B**, FKBP-AKAR3 and SR-AKAR3 biosensors were expressed in AVMs isolated from mice after chronic infusion of saline or isoproterenol (CM). Dot plots show the maximal YFP/CFP ratio of FKBP-AKAR3 and SR-AKAR3 in AVMs after stimulation with norepinephrine (1  $\mu$ mol/L) alone or in the presence of monoamine oxidase A inhibitor (MAOi, clorgyline, 5  $\mu$ mol/L). *P* values were obtained using 2-way ANOVA followed by Tukey's test. **C through G**, AVMs were loaded with fluo-4 AM dye and paced at 1 Hz. AVMs were then stimulated with norepinephrine (1  $\mu$ mol/L) alone or in the presence of MAOi (5  $\mu$ mol/L). CaT decay tau and amplitude and SS were recorded in AVMs after stimulation with norepinephrine. Representative traces show calcium transient and sarcomere shortening. Dot plots show maximal CaT amplitude and decay tau and SS in AVMs after stimulation. Dot plots representing mean  $\pm$  SEM of AVMs from 6 mice. *P* values were obtained using 2-way ANOVA followed by Tukey's test. **H and I**, Working model of the subcellular  $\beta_1$ AR signaling desensitization under chronic adrenergic stress. Cardiac  $\beta_1$ AR is downregulated at the local RyR2 nanodomains in the mouse cardiomyopathy induced by chronic infusion of isoproterenol. In comparison, MAO-A-mediated restriction of the access of catecholamines to the  $\beta_1$ AR at the SERCA2a nanodomains leads to impaired local signaling in the mouse cardiomyopathy induced by chronic infusion of isoproterenol. AVM indicates adult ventricular myocyte;  $\beta_1$ AR,  $\beta_1$  adrenergic receptor; CaT, calcium transient; CFP, cyan fluorescent protein; Cilo, cilostamide; CM, cardiomyopathy; E-C, excitation-contraction; EHNA, erythro-9-(2-hydroxy-3-nonyl) adenine; FKBP-AKAR3, FK506 binding protein 12.6 anchored a kinase activity reporter 3; FSK, forskolin; IBMX, isobutylmethylxanthine; LTCC, L-type calcium channel; MAO-A monoamine oxidase A; MAOi, monoamine oxidase inhibitor; NE, norepinephrine; PDE4D, phosphodiesterase 4D; PKA, protein kinase A; Roli, rolipram; RyR2, ryanodine receptor 2; Sal, saline; SERCA2a, (Sarco)endoplasmic reticulum calcium ATPase 2a; SR-AKAR3, sarcoplasmic reticulum anchored a kinase activity reporter 3; SS, sarcomere shortening; tau, taurine; and YFP, yellow fluorescent protein.



The biosensors offer great advantages in probing the dynamic local signaling in AVMs, and our AKAR3 biosensors have been extensively characterized previously.<sup>22,23,27</sup> However, the biosensor detection has

several limitations. One caveat is that they may be mistargeted when overexpressed in AVMs. We should also be more cautious when probing AVMs from mice after chronic isoproterenol infusion, which may have

altered membrane structure, such as T-tubules.<sup>47</sup> We could not rule out the possibility that these biosensors detect minor signals from unintended locations along the secretory pathways. Therefore, FRET data should be corroborated with cellular, biochemical, and functional data. Meanwhile, due to the complexity of the distribution of individual channels and transporters on membrane structures, our study is limited to its biochemical nature and does not address morphological and signaling alterations in individual membrane structures in AVMs.

## CONCLUSION

Nevertheless, in this study, our data collectively support distinct remodeling of adrenergic signaling at the RyR2 and SERCA2a complexes in mouse cardiomyopathy after a chronic infusion of isoproterenol. Our study offers strategies to restore the subcellular cardiac  $\beta$ <sub>1</sub>AR signaling and contractile function in cardiomyopathy associated with chronic sympathetic stress.

## ARTICLE INFORMATION

Received November 29, 2023; accepted May 15, 2024.

### Affiliations

VA Northern California Health Care System, Mather, CA (B.X., Y.K.X.); Department of Pharmacology, University of California at Davis, Davis, CA (B.X., S.B., V.R.S., Y.W., C.Z., M.Z., Y.K.X.); Department of Clinical Pathology, Faculty of Medicine, Mansoura University, Mansoura, Egypt (S.B.); Department of Pharmacology, School of Medicine, Southern University of Science and Technology, Shenzhen, China (Y.W.); and Department of Pharmaceutical Toxicology, China Medical University, Shenyang, China (M.Z.).

### Acknowledgments

Bing Xu, Ying Wang, and Yang K. Xiang conceived the idea and designed the experiments; Bing Xu, Ying Wang, Sherif Bahriz, Victoria R. Salemme, Chaoqun Zhu, and Meimi Zhao acquired and analyzed the data, Bing Xu finalized the figures and Yang K. Xiang wrote and revised the article.

### Sources of Funding

This work was supported by National Institutes of Health grants R01-HL147263 and HL162825, Veteran Affairs Merit grants IK6BX005753, 01BX002900 and BX005100 (Yang K. Xiang). Ying Wang and Chaoqun Zhu are recipients of American Heart Association postdoctoral fellowship. Yang K. Xiang is an established American Heart Association investigator.

### Disclosures

None.

### Supplemental Material

Tables S1–S2

## REFERENCES

- Rapacciuolo A, Suvarna S, Barki-Harrington L, Luttrell LM, Cong M, Lefkowitz RJ, Rockman HA. Protein kinase a and G protein-coupled receptor kinase phosphorylation mediates beta-1 adrenergic receptor endocytosis through different pathways. *J Biol Chem*. 2003;278:35403–35411. doi: [10.1074/jbc.M305675200](https://doi.org/10.1074/jbc.M305675200)
- Naga Prasad SV, Laporte SA, Chamberlain D, Caron MG, Barak L, Rockman HA. Phosphoinositide 3-kinase regulates beta2-adrenergic receptor endocytosis by AP-2 recruitment to the receptor/beta-arrestin complex. *J Cell Biol*. 2002;158:563–575. doi: [10.1083/jcb.200202113](https://doi.org/10.1083/jcb.200202113)
- Xu B, Li M, Wang Y, Zhao M, Morotti S, Shi Q, Wang Q, Barbagallo F, Teoh JP, Reddy GR, et al. GRK5 controls SAP97-dependent cardiotoxic beta1 adrenergic receptor-CaMKII signaling in heart failure. *Circ Res*. 2020;127:796–810. doi: [10.1161/CIRCRESAHA.119.316319](https://doi.org/10.1161/CIRCRESAHA.119.316319)
- Wang Y, Shi Q, Li M, Zhao M, Reddy Gopireddy R, Teoh JP, Xu B, Zhu C, Ireton KE, Srinivasan S, et al. Intracellular beta1-adrenergic receptors and organic cation transporter 3 mediate phospholamban phosphorylation to enhance cardiac contractility. *Circ Res*. 2021;128:246–261. doi: [10.1161/CIRCRESAHA.120.317452](https://doi.org/10.1161/CIRCRESAHA.120.317452)
- Wang Y, Zhao M, Shi Q, Xu B, Zhu C, Li M, Mir V, Bers DM, Xiang YK. Monoamine oxidases desensitize intracellular beta1AR signaling in heart failure. *Circ Res*. 2021;129:965–967. doi: [10.1161/CIRCRESAHA.121.319546](https://doi.org/10.1161/CIRCRESAHA.121.319546)
- Wang Y, Zhao M, Xu B, Bahriz SMF, Zhu C, Jovanovic A, Ni H, Jacobi A, Kaludercic N, Di Lisa F, et al. Monoamine oxidase a and organic cation transporter 3 coordinate intracellular beta1AR signaling to calibrate cardiac contractile function. *Basic Res Cardiol*. 2022;117:37. doi: [10.1007/s00395-022-00944-5](https://doi.org/10.1007/s00395-022-00944-5)
- Bers DM, Fill M. Coordinated feet and the dance of ryanodine receptors. *Science*. 1998;281:790–791. doi: [10.1126/science.281.5378.790](https://doi.org/10.1126/science.281.5378.790)
- Bers DM. Cardiac excitation-contraction coupling. *Nature*. 2002;415:198–205. doi: [10.1038/415198a](https://doi.org/10.1038/415198a)
- Zaccolo M, Zerio A, Lobo MJ. Subcellular organization of the cAMP signaling pathway. *Pharmacol Rev*. 2021;73:278–309. doi: [10.1124/pharmrev.120.000086](https://doi.org/10.1124/pharmrev.120.000086)
- Ercu M, Klussmann E. Roles of A-kinase anchoring proteins and Phosphodiesterases in the cardiovascular system. *J Cardiovasc Dev Dis*. 2018;5:14. doi: [10.3390/jcdd5010014](https://doi.org/10.3390/jcdd5010014)
- Lin TY, Mai QN, Zhang H, Wilson E, Chien HC, Yee SW, Giacomini KM, Olgin JE, Irannejad R. Cardiac contraction and relaxation are regulated by distinct subcellular cAMP pools. *Nat Chem Biol*. 2023;20:62–73. doi: [10.1038/s41589-023-01381-8](https://doi.org/10.1038/s41589-023-01381-8)
- Nash CA, Wei W, Irannejad R, Smrcka AV. Golgi localized beta1-adrenergic receptors stimulate Golgi PI4P hydrolysis by PLCepsilon to regulate cardiac hypertrophy. *elife*. 2019;8:e48167. doi: [10.7554/eLife.48167](https://doi.org/10.7554/eLife.48167)
- Richter W, Day P, Agrawal R, Bruss MD, Granier S, Wang YL, Rasmussen SG, Horner K, Wang P, Lei T, et al. Signaling from beta1- and beta2-adrenergic receptors is defined by differential interactions with PDE4. *EMBO J*. 2008;27:384–393. doi: [10.1038/sj.emboj.7601968](https://doi.org/10.1038/sj.emboj.7601968)
- Xiang Y, Naro F, Zoudilova M, Jin SL, Conti M, Kobilka B. Phosphodiesterase 4D is required for {beta}2 adrenoceptor subtype-specific signaling in cardiac myocytes. *Proc Natl Acad Sci USA*. 2005;102:909–914. doi: [10.1073/pnas.0405263102](https://doi.org/10.1073/pnas.0405263102)
- De Arcangelis V, Liu R, Soto D, Xiang Y. Differential association of phosphodiesterase 4D isoforms with beta2-adrenoceptor in cardiac myocytes. *J Biol Chem*. 2009;284:33824–33832. doi: [10.1074/jbc.M109.020388](https://doi.org/10.1074/jbc.M109.020388)
- Fu Q, Kim S, Soto D, De Arcangelis V, DiPillato L, Liu S, Xu B, Shi Q, Zhang J, Xiang YK. A long lasting beta1 adrenergic receptor stimulation of cAMP/protein kinase A (PKA) signal in cardiac myocytes. *J Biol Chem*. 2014;289:14771–14781. doi: [10.1074/jbc.M113.542589](https://doi.org/10.1074/jbc.M113.542589)
- Lehnart SE, Wehrens XH, Reiken S, Warriar S, Belevych AE, Harvey RD, Richter W, Jin SL, Conti M, Marks AR. Phosphodiesterase 4D deficiency in the ryanodine-receptor complex promotes heart failure and arrhythmias. *Cell*. 2005;123:25–35. doi: [10.1016/j.cell.2005.07.030](https://doi.org/10.1016/j.cell.2005.07.030)
- Beca S, Helli PB, Simpson JA, Zhao D, Farman GP, Jones PP, Tian X, Wilson LS, Ahmad F, Chen SR, et al. Phosphodiesterase 4D regulates baseline sarcoplasmic reticulum Ca2+ release and cardiac contractility, independently of L-type Ca2+ current. *Circ Res*. 2011;109:1024–1030. doi: [10.1161/CIRCRESAHA.111.250464](https://doi.org/10.1161/CIRCRESAHA.111.250464)
- Movsesian M, Ahmad F, Hirsch E. Functions of PDE3 isoforms in cardiac muscle. *J Cardiovasc Dev Dis*. 2018;5:10. doi: [10.3390/jcdd5010010](https://doi.org/10.3390/jcdd5010010)
- Ahmad F, Shen W, Vandeput F, Szabo-Fresnais N, Krall J, Degerman E, Goetz F, Klussmann E, Movsesian M, Manganiello V. Regulation of sarcoplasmic reticulum Ca2+ ATPase 2 (SERCA2) activity by phosphodiesterase 3A (PDE3A) in human myocardium: phosphorylation-dependent interaction of PDE3A1 with SERCA2. *J Biol Chem*. 2015;290:6763–6776. doi: [10.1074/jbc.M115.638585](https://doi.org/10.1074/jbc.M115.638585)



21. Singh A, Redden JM, Kapiloff MS, Dodge-Kafka KL. The large isoforms of A-kinase anchoring protein 18 mediate the phosphorylation of inhibitor-1 by protein kinase A and the inhibition of protein phosphatase 1 activity. *Mol Pharmacol*. 2011;79:533–540. doi: [10.1124/mol.110.065425](https://doi.org/10.1124/mol.110.065425)
22. Liu S, Li Y, Kim S, Fu Q, Parikh D, Sridhar B, Shi Q, Zhang X, Guan Y, Chen X, et al. Phosphodiesterases coordinate cAMP propagation induced by two stimulatory G protein-coupled receptors in hearts. *Proc Natl Acad Sci USA*. 2012;109:6578–6583. doi: [10.1073/pnas.1117862109](https://doi.org/10.1073/pnas.1117862109)
23. Liu SB, Zhang J, Xiang YK. FRET-based direct detection of dynamic protein kinase A activity on the sarcoplasmic reticulum in cardiomyocytes. *BBRC*. 2010;404:581–586.
24. Xu B, Wang Y, Bahriz SMF, Zhao M, Zhu C, Xiang YK. Probing spatio-temporal PKA activity at the ryanodine receptor and SERCA2a nanodomains in cardiomyocytes. *Cell Commun Signal*. 2022;20:143. doi: [10.1186/s12964-022-00947-8](https://doi.org/10.1186/s12964-022-00947-8)
25. Wang Q, Liu Y, Fu Q, Xu B, Zhang Y, Kim S, Tan R, Barbagallo F, West T, Anderson E, et al. Inhibiting insulin-mediated beta2-adrenergic receptor activation prevents diabetes-associated cardiac dysfunction. *Circulation*. 2017;135:73–88. doi: [10.1161/CIRCULATIONAHA.116.022281](https://doi.org/10.1161/CIRCULATIONAHA.116.022281)
26. Zhang X, Szeto C, Gao E, Tang M, Jin J, Fu Q, Makarewich C, Ai X, Li Y, Tang A, et al. Cardiotoxic and cardioprotective features of chronic beta-adrenergic signaling. *Circ Res*. 2013;112:498–509. doi: [10.1161/CIRCRESAHA.112.273896](https://doi.org/10.1161/CIRCRESAHA.112.273896)
27. Soto D, De Arcangelis V, Zhang J, Xiang Y. Dynamic protein kinase A activities induced by beta-adrenoceptors dictate signaling propagation for substrate phosphorylation and myocyte contraction. *Circ Res*. 2009;104:770–779. doi: [10.1161/CIRCRESAHA.108.187880](https://doi.org/10.1161/CIRCRESAHA.108.187880)
28. Barbagallo F, Xu B, Reddy GR, West T, Wang Q, Fu Q, Li M, Shi Q, Ginsburg KS, Ferrier W, et al. Genetically encoded biosensors reveal PKA hyperphosphorylation on the myofilaments in rabbit heart failure. *Circ Res*. 2016;119:931–943. doi: [10.1161/CIRCRESAHA.116.308964](https://doi.org/10.1161/CIRCRESAHA.116.308964)
29. Buonarati OR, Henderson PB, Murphy GG, Horne MC, Hell JW. Proteolytic processing of the L-type Ca(2+) channel alpha(1)1.2 subunit in neurons. *F1000Res*. 2017;6:1166. doi: [10.12688/f1000research.11808.1](https://doi.org/10.12688/f1000research.11808.1)
30. Agrawal V, Fortune N, Yu S, Fuentes J, Shi F, Nichols D, Gleaves L, Poovey E, Wang TJ, Brittain EL, et al. Natriuretic peptide receptor C contributes to disproportionate right ventricular hypertrophy in a rodent model of obesity-induced heart failure with preserved ejection fraction with pulmonary hypertension. *Pulm Circ*. 2019;9:2045894019878599. doi: [10.1177/2045894019878599](https://doi.org/10.1177/2045894019878599)
31. Zhang H, Makarewich CA, Kubo H, Wang W, Duran JM, Li Y, Berretta RM, Koch WJ, Chen X, Gao E, et al. Hyperphosphorylation of the cardiac ryanodine receptor at serine 2808 is not involved in cardiac dysfunction after myocardial infarction. *Circ Res*. 2012;110:831–840. doi: [10.1161/CIRCRESAHA.111.255158](https://doi.org/10.1161/CIRCRESAHA.111.255158)
32. Xiao H, Li H, Wang JJ, Zhang JS, Shen J, An XB, Zhang CC, Wu JM, Song Y, Wang XY, et al. IL-18 cleavage triggers cardiac inflammation and fibrosis upon beta-adrenergic insult. *Eur Heart J*. 2018;39:60–69. doi: [10.1093/eurheartj/ehx261](https://doi.org/10.1093/eurheartj/ehx261)
33. Zhu J, Steinberg SF. Beta(1)-adrenergic receptor cleavage and regulation by elastase. *JACC Basic Transl Sci*. 2023;8:976–988. doi: [10.1016/j.jacbs.2023.02.002](https://doi.org/10.1016/j.jacbs.2023.02.002)
34. Berisha F, Gotz KR, Wegener JW, Brandenburg S, Subramanian H, Molina CE, Ruffer A, Petersen J, Bernhardt A, Girdauskas E, et al. cAMP imaging at ryanodine receptors reveals beta2-adrenoceptor driven arrhythmias. *Circ Res*. 2021;129:81–94. doi: [10.1161/CIRCRESAHA.120.318234](https://doi.org/10.1161/CIRCRESAHA.120.318234)
35. Kaludercic N, Takimoto E, Nagayama T, Feng N, Lai EW, Bedja D, Chen K, Gabrielson KL, Blakely RD, Shih JC, et al. Monoamine oxidase A-mediated enhanced catabolism of norepinephrine contributes to adverse remodeling and pump failure in hearts with pressure overload. *Circ Res*. 2010;106:193–202. doi: [10.1161/CIRCRESAHA.109.198366](https://doi.org/10.1161/CIRCRESAHA.109.198366)
36. Manni ME, Rigacci S, Borchini E, Bargelli V, Miceli C, Giordano C, Raimondi L, Nediani C. Monoamine oxidase is overactivated in left and right ventricles from ischemic hearts: An intriguing therapeutic target. *Oxidative Med Cell Longev*. 2016;2016:4375418. doi: [10.1155/2016/4375418](https://doi.org/10.1155/2016/4375418)
37. Huang B, Wang S, Qin D, Boutjdir M, El-Sherif N. Diminished basal phosphorylation level of phospholamban in the postinfarction remodeled rat ventricle: role of beta-adrenergic pathway, G(i) protein, phosphodiesterase, and phosphatases. *Circ Res*. 1999;85:848–855. doi: [10.1161/01.RES.85.9.848](https://doi.org/10.1161/01.RES.85.9.848)
38. Wang W, Zhu W, Wang S, Yang D, Crow MT, Xiao RP, Cheng H. Sustained beta1-adrenergic stimulation modulates cardiac contractility by Ca2+/calmodulin kinase signaling pathway. *Circ Res*. 2004;95:798–806. doi: [10.1161/01.RES.0000145361.50017.aa](https://doi.org/10.1161/01.RES.0000145361.50017.aa)
39. Zhang T, Guo T, Mishra S, Dalton ND, Kranias EG, Peterson KL, Bers DM, Brown JH. Phospholamban ablation rescues sarcoplasmic reticulum Ca(2+) handling but exacerbates cardiac dysfunction in CaMKIIdelta(C) transgenic mice. *Circ Res*. 2010;106:354–362. doi: [10.1161/CIRCRESAHA.109.207423](https://doi.org/10.1161/CIRCRESAHA.109.207423)
40. Ai X, Curran JW, Shannon TR, Bers DM, Pogwizd SM. Ca2+/calmodulin-dependent protein kinase modulates cardiac ryanodine receptor phosphorylation and sarcoplasmic reticulum Ca2+ leak in heart failure. *Circ Res*. 2005;97:1314–1322. doi: [10.1161/01.RES.0000194329.41863.89](https://doi.org/10.1161/01.RES.0000194329.41863.89)
41. Pereira L, Cheng H, Lao DH, Na L, van Oort RJ, Brown JH, Wehrens XH, Chen J, Bers DM. Epac2 mediates cardiac beta1-adrenergic-dependent sarcoplasmic reticulum Ca2+ leak and arrhythmia. *Circulation*. 2013;127:913–922. doi: [10.1161/CIRCULATIONAHA.12.148619](https://doi.org/10.1161/CIRCULATIONAHA.12.148619)
42. Williams LT, Jones LR. Specific binding of the calcium antagonist [3H] nitrendipine to subcellular fractions isolated from canine myocardium. Evidence for high affinity binding to ryanodine-sensitive sarcoplasmic reticulum vesicles. *J Biol Chem*. 1983;258:5344–5347. doi: [10.1016/S0021-9258\(20\)81893-6](https://doi.org/10.1016/S0021-9258(20)81893-6)
43. Perrino C, Naga Prasad SV, Schroder JN, Hata JA, Milano C, Rockman HA. Restoration of beta-adrenergic receptor signaling and contractile function in heart failure by disruption of the betaARK1/phosphoinositide 3-kinase complex. *Circulation*. 2005;111:2579–2587. doi: [10.1161/CIRCULATIONAHA.104.508796](https://doi.org/10.1161/CIRCULATIONAHA.104.508796)
44. Toma M, Starling RC. Inotropic therapy for end-stage heart failure patients. *Curr Treat Options Cardiovasc Med*. 2010;12:409–419. doi: [10.1007/s11936-010-0090-9](https://doi.org/10.1007/s11936-010-0090-9)
45. Maack C, Eschenhagen T, Hamdani N, Heinzel FR, Lyon AR, Manstein DJ, Metzger J, Papp Z, Tocchetti CG, Yilmaz MB, et al. Treatments targeting inotropy. *Eur Heart J*. 2019;40:3626–3644. doi: [10.1093/eurheartj/ehy600](https://doi.org/10.1093/eurheartj/ehy600)
46. Bellinger AM, Reiken S, Dura M, Murphy PW, Deng SX, Landry DW, Nieman D, Lehnart SE, Samaru M, LaCampaña A, et al. Remodeling of ryanodine receptor complex causes "leaky" channels: a molecular mechanism for decreased exercise capacity. *Proc Natl Acad Sci USA*. 2008;105:2198–2202. doi: [10.1073/pnas.0711074105](https://doi.org/10.1073/pnas.0711074105)
47. Guo A, Zhang C, Wei S, Chen B, Song LS. Emerging mechanisms of T-tubule remodeling in heart failure. *Cardiovasc Res*. 2013;98:204–215. doi: [10.1093/cvr/cvt020](https://doi.org/10.1093/cvr/cvt020)